Design of a super directive four-element compact antenna array using spherical wave expansion

Antonio Clemente, Mélusine Pigeon, Lionel Rudant, Christophe Delaveaud

HAL Id: cea-03637151

https://cea.hal.science/cea-03637151

Submitted on 11 Apr 2022

Design of a Super Directive Four-Element Compact Antenna Array Using Spherical Wave Expansion

Antonio Clemente, *Member, IEEE,* Melusine Pigeon, Lionel Rudant, and Christophe Delaveaud, *Member, IEEE*

Abstract—In this paper, a super directive four-element compact parasitic antenna array has been designed and optimized using an *ad hoc* procedure based on the Harrington maximum directivity definition and spherical wave expansion. The complete design procedure (i.e. calculation of the optimum excitation coefficients and equivalent impedance loads associated to each parasitic element) is presented and validated through full-wave electromagnetic simulations. The proposed array has been designed at 868 MHz; its electrical size is $0.45\lambda_0 \times 0.36\lambda_0$ (diameter of minimum sphere circumscribing the antenna equal to $0.57\lambda_0$). A prototype has been built and tested to demonstrate the effectiveness of this design. A maximum directivity of 11.7 dBi has been measured at 871 MHz in satisfactory agreement with theoretical results and electromagnetic simulations.

Index Terms—Super directivity, compact antenna, parasitic antenna array, antenna directivity optimization.

I. INTRODUCTION

DIRECTIVE compact antennas offer new opportunities for wireless applications in terms of spectral efficiency, reduced environmental impact and use modes. However, the conventional techniques for enhancing the directivity often lead to a significant increase of the antenna size. Consequently, the integration of directional antennas in small wireless devices is relatively limited. This difficulty is particularly critical for the frequency bands below 1 GHz if object dimensions are limited to a few centimeters. With the explosion of the number of wireless communication systems (WiFi wireless networks, RFID tags, wireless sensor networks, object remote control, connected objects, etc.), the problem of electromagnetic pollution has also emerged. The necessary management of interferences limits the spectral efficiency of wireless communications, thus reducing the communication performance and autonomy of battery-operated system. Super directive compact antennas are an innovative and attractive solution to both integration and interference mitigation needs.

The relationship between antenna size and maximum normal directivity has been discussed in several works [1]-[2]. Harrington [1] has shown that the maximum normal directivity of an antenna enclosed in a minimum sphere of radius r_0 can approach to $N^2 + 2N$, where $N = kr_0$ is the maximum degree of the spherical wave expansion of the

radiated field and k is the wavenumber. A useful definition of antenna super directivity is directivity higher than that obtained with the same antenna size considering the Harrington normal directivity limit.

Compact antennas have been largely studied in terms of quality factor, bandwidth, radiation efficiency, and matching properties [3]-[11]. Due to their reduced electrical size, they typically radiate an omnidirectional pattern. Therefore, one of the most challenging research topics in antenna design is to achieve directional patterns using electrically small antennas. In 1946, Uzkov [12] has shown that the maximum end-fire directivity of a linear array of N_A isotropic radiators approaches to N_A^2 when the inter-element distance vanishes (e.g. the end-fire directivity attains to 6.0, 9.5, and 12.0 dBi for a two-, three-, and four-element array, respectively). Using elementary electric or magnetic dipoles, the theoretical maximum directivity has been numerically estimated in [13] and is equal to 7.2, 10.3, and 12.6 dBi in the case of a two-, three-, and four-element array, respectively.

Several proofs of concept of directive compact antennas have been presented in the open literature [14]-[19], but major theoretical and practical aspects are not yet studied (e.g. practical antenna implementation, design procedure, radiation efficiency, etc.). To our best knowledge, any practical demonstration of four-element (or more) antenna array has not been presented in the open literature. An exhaustive state of the art on super directive antennas is presented in [20].

In this work, a procedure for the design of super directive antenna arrays is demonstrated. The directivity performances of several fixed size arrays (three-, four-, five-, and seven-element) have been theoretically studied. The impact of the super directivity on the radiation efficiency of the four-element array has also been investigated as a function of the inter-element distance. Then, the proposed method has been applied for the optimization of a super directive four-element parasitic antenna array working at 868 MHz. Our objective is to get the highest directivity with a compact antenna to obtain an efficient spatial filtering function independently from the power efficiency.

The paper is organized as follows. In Section II, the theoretical background is presented. Then, the complete optimization procedure is described in Section III. In this section, a theoretical analysis is also proposed and validated by full-wave simulations. The proposed super directive array and its experimental characterization are presented in Section IV. Finally, conclusions are drawn in Section V. Preliminary results of this work were presented in [21].

A. Clemente, M. Pigeon, L. Rudant, and C. Delaveaud are with CEA-LETI, Minatec Campus, F38054 Grenoble, France (e-mail: antonio.clemente@cea.fr, lionel.rudant@cea.fr, christophe.delaveaud@cea.fr).

II. THEORETICAL BACKGROUND

A. Spherical wave expansion

The electric field $\vec{E}$ at large distance ($kr \rightarrow \infty$) outside an enclosing spherical surface including all the field sources can be represented as a linear combination of far-field spherical wave pattern functions $\vec{K}_{smn}(\theta,\phi)$ [22]

$$
\begin{aligned}
\vec{E}(r,\theta,\phi) &= \sqrt{\eta}\,\frac{k}{\sqrt{4\pi}}\,\frac{e^{ikr}}{kr}\sum_{s=1}^{2}\sum_{n=1}^{N}\sum_{m=-n}^{n}Q_{smn}\vec{K}_{smn}(\theta,\phi) \\
&= \sqrt{\eta}\,\frac{k}{\sqrt{4\pi}}\,\frac{e^{ikr}}{kr}\sum_{smn}Q_{smn}\vec{K}_{smn}(\theta,\phi)
\end{aligned}
,\qquad (1)
$$

where η is the specific impedance of the medium assumed complex, and Q_{smn} are the spherical wave coefficients. The degree n is equal to $1,2,\ldots,N$ and the order is limited by $|m| \leq n$. The index $s = 1,2$ indicates a coefficient to a TE- and a TM-mode wave, respectively. The wave pattern functions $\vec{K}_{smn}(\theta,\phi)$ are dimensionless and are solution of the Helmholtz wave equation. Their explicit definition is

$$
\begin{aligned}
\vec{K}_{1mn}(\theta,\phi) &= \sqrt{\frac{2}{n(n+1)}}\left(-\frac{m}{|m|}\right)^m e^{jm\phi}(-j)^{n+1} \\
&\left\{\frac{jm\overline{P}_n^{|m|}(\cos\theta)}{\sin\theta}\vec{e}_\theta - \frac{d\overline{P}_n^{|m|}(\cos\theta)}{d\theta}\vec{e}_\phi\right\}
\end{aligned}
,\quad (2a)
$$

$$
\begin{aligned}
\vec{K}_{2mn}(\theta,\phi) &= \sqrt{\frac{2}{n(n+1)}}\left(-\frac{m}{|m|}\right)^m e^{jm\phi}(-j)^n \\
&\left\{\frac{d\overline{P}_n^{|m|}(\cos\theta)}{d\theta}\vec{e}_\theta + \frac{jm\overline{P}_n^{|m|}(\cos\theta)}{\sin\theta}\vec{e}_\phi\right\}
\end{aligned}
,\quad (2b)
$$

where $\overline{P}_n^m(\cos\theta)$ is the normalized associated Legendre function.

The terms Q_{smn} can be calculated from equation (1) using the orthogonal properties of the spherical wave functions [22] or matrix inversion techniques ([23], p. 31).

B. Spherical wave truncation criteria

The electric field radiated by a generic source enclosed in a minimum sphere of radius r_0 and expressed as a linear combination of spherical wave functions (1), is in principle of infinite degree n [22]. Consequently, in agreement with Harrington definition [1], the directivity of an antenna is in theory infinite ($N \rightarrow \infty$). However, considering the spherical wave radial function [22], a transition point between propagation and evanescence can be defined for each mode of degree n around a radial distance $r_t = n/k$. This concept has been presented in several works [1],[22]. In accord with Harrington's observation [1], the spherical modes with $n > kr$ are highly attenuated outside the minimum sphere and only modes with $n < kr$ contribute to the radiated far-field. In practice, the degree n can be truncated at some $n = N$, with $N = kr_0 + n_1$ [22]. The value n_1 depends on the desired accuracy and on the definition of the coordinate system [22]-[24].

In the proposed design procedure, the number of spherical modes N used for the optimization is defined considering the radiation power of each array element (P_{rad}^p) and is fixed as $N \in \mathrm{N}^+ | P_{rad}^p = 99.9\%$, where N^+ are the natural numbers excluding the zero.

C. Maximum directivity

Starting from its definition and the far-field expression (1), the directivity $D(\theta,\phi)$ can be calculated as [22]

$$
D(\theta,\phi) = \frac{\left|\sum_{smn}Q_{smn}\vec{K}_{smn}(\theta,\phi)\right|^2}{\sum_{smn}|Q_{smn}|^2} . \qquad (3)
$$

In 1958, Harrington [1] established a limit on the maximum attainable directivity in a given direction (θ_0,ϕ_0) depending on the number of spherical modes associated to the antenna radiation when wave functions up to $n = N$ are included. This limit can be easily calculated applying the Cauchy-Schwartz inequality on equation (3)

$$
\begin{aligned}
D_{\max}(\theta_0,\phi_0) &= \sum_{smn}\left|\vec{K}_{smn}(\theta_0,\phi_0)\cdot\hat{i}^*\right|^2 \\
&= \sum_{n=1}^{N}(2n+1) \\
&= N^2 + 2N
\end{aligned}
,\qquad (4)
$$

where $\hat{i}$ represents the reference polarization and the symbol * indicates the complex and conjugate operation. Due to the properties of spherical wave functions, the maximum order N is independent of rotation ([22], p. 343). Therefore, the maximum directivity is independent of the direction (θ_0,ϕ_0) and the chosen polarization. As presented in [22], if all modes N can be weighted separately, the maximum directivity can be obtained if

$$
Q_{smn}^{\max} = c \cdot \vec{K}_{smn}^*(\theta_0,\phi_0) , \qquad (5)
$$

where c is an arbitrary constant, which has been calculated by applying the conservation of energy principle. In fact, from the spherical wave expansion theory it is well known that the radiated power can be calculated from the spherical wave coefficients as [22]

$$
P_{rad} = \frac{1}{2}\sum_{smn}|Q_{smn}|^2 . \qquad (6)
$$

Using in (6) the maximum directivity spherical wave coefficients $Q_{smn}^{\max}$ (5) and imposing $P_{rad} = 1$ W it is possible to calculate the c constant as

$$
c = \sqrt{\frac{2}{\sum_{smn}\left|\vec{K}_{smn}^*(\theta_0,\phi_0)\right|^2}} . \qquad (7)
$$

III. SUPER DIRECTIVE PARASITIC ARRAYS SYNTHESIS PROCEDURE

In this section, the complete parasitic array synthesis procedure is discussed. The main interest of the proposed design is to avoid the size and complexity of the feed network. Thus, only one antenna element is fed, while the others are connected to impedance loads and electromagnetically coupled. The aim of the proposed procedure is to find the optimal weights and the equivalent impedance loads (combination of resistive and reactive loads) needed to achieve the maximum directivity in a desired direction. The schematic diagram of the procedure is presented in Fig. 1, it consists of four steps.
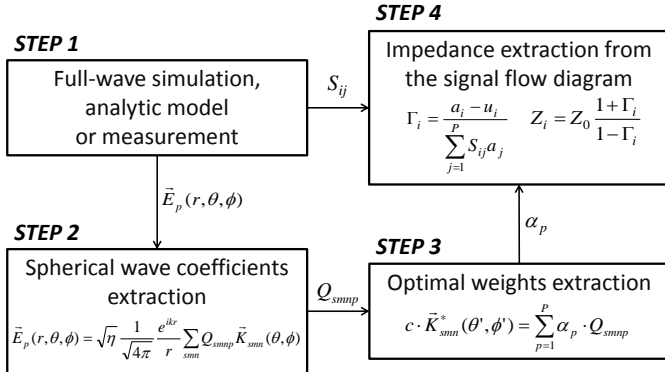

Fig. 1. Schematic diagram of the proposed parasitic array optimization procedure.

A. Mutual coupling and input impedance

Due to the reduced distance between the array elements, the mutual coupling effects must be taken into account for an accurate design of compact array antennas [25]. Therefore, in the array factor the active element patterns are included. As presented in [26],[27], an active element pattern can be calculated by feeding only the antenna p with a normalized power, while the others array elements $i \neq p$ are connected to a port impedance $Z_i = 50\ \Omega$.

In the STEP 1 of the synthesis procedure, the elementary electric far-field ($\vec{E}_p(r,\theta,\phi)$) of each array element and the scattering matrix have been calculated using CST Microwave Studio. Then, the simulated elementary electric far-fields are used in the STEP 2 in order to calculate the associated spherical wave coefficients using (1).

B. Optimal excitation coefficients extraction

Solving equation (5), the spherical wave coefficients needed to maximize the directivity can be extracted when all modes are independently excited. Instead, for a P-element array, each element presents a fixed number $2N(N + 1)$ of spherical modes (1) which cannot be independently excited. In other words, in this case, the same excitation coefficient (α_p) must be applied on a mode series associated to a single array element.

$$
\begin{aligned}
Q_{smn}^{\max} &= c \cdot \vec{K}_{smn}^{*}(\theta_0,\phi_0) \\
&= \sum_{p=1}^{P} \alpha_p \cdot Q_{smnp}
\end{aligned}
\tag{8}
$$

where Q_{smnp} are the spherical wave coefficients associated to the p element calculated in the STEP 2 of the procedure.

Writing (8) in vector form, we can compute the terms α_p as (STEP 3)

$$
\overline{\alpha} = \overline{\overline{Q}}^{+}\,\overline{K} ,
\tag{9}
$$

where $\overline{\alpha}$ is the unknown column vector containing the p excitation coefficients, $\overline{K}$ is a column vector containing $2N(N + 1)$ terms calculated from $\vec{K}_{smn}^{*}(\theta_0,\phi_0)$, and $\overline{\overline{Q}}$ is a $p \times 2N(N + 1)$ matrix containing the terms Q_{smnp}. The symbol $^{+}$ indicates the pseudo inverse operation.

Since, the total radiated electric far-field of the array can be expressed as a weighted combination of the electric far-field $\vec{E}_p(\theta,\phi)$ radiated by each element [26],[27]

$$
\vec{E}(\theta,\phi) = \sum_{p=1}^{P} \alpha_p \vec{E}_p(\theta,\phi) ,
\tag{10}
$$

the array directivity can be easily calculated as

$$
D(\theta,\phi) = \frac{\left| \sum_{p=1}^{P} \alpha_p \sum_{smn} Q_{smnp} \vec{K}_{smn}(\theta,\phi) \right|^2}{\sum_{smn} \left| \sum_{p=1}^{P} \alpha_p Q_{smnp} \right|^2} .
\tag{11}
$$

C. Theoretical results

A theoretical analysis has been computed at 868 MHz considering four different compact arrays of constant size ($0.4\lambda_0 \times 0.2\lambda_0$, $r_0 = 0.22\lambda_0$). The array are printed on the Rogers RO4003 substrate ($\varepsilon_r = 3.55$ and $\tan\delta = 0.0027$, and thickness equal to 813 µm). They are respectively composed of three, four, five, and seven identical uniformly spaced electrical dipoles of thickness $\sim 0.01\lambda_0$ mm and electrical length $0.4\lambda_0$. A schematic view of a generic array is presented in Fig. 2(a). The directivity has been optimized in the end-fire direction ($\theta_0 = 90°, \phi_0 = 0$). The flow diagram representation of a generic two-element array is also presented in Fig. 2(b).
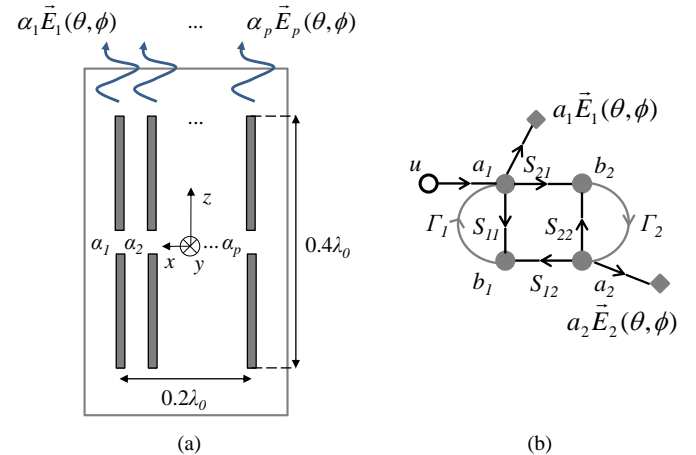

Fig. 2. Principle of a parasitic antenna array. (a) Schematic view of a p-element array and (b) flow diagram of a two-element array.

In order to consider the mutual coupling effects between each array element (Section II.A), the four antennas have been simulated using CST Microwave Studio. Then, the simulated complex electric far-fields $\vec{E}_p(r,\theta,\varphi)$ have been used to calculate the optimal excitation coefficients from (7)-(9). Finally, the theoretical and simulated directivity has been computed using the optimal excitation coefficients in (11) and in CST Microwave Studio, respectively.

TABLE I

THEORETICAL AND SIMULATED DIRECTIVITY OF THE THREE-, FOUR-, FIVE-, AND SEVEN-ELEMENT ARRAY OPTIMIZED AT 868 MHz.

N. of elements	Inter-element distance (λ_0)	N	Directivity maximum (dBi) [13]	Theoretical directivity (dBi)	Simulated. directivity (dBi)
3	0.1	5	10.3	10.4	10.3
4	0.07	5	12.6	12.5	12.7
5	0.05	5	14.4	13.8	13.9
7	0.03	6	17.2	14.3	15.4

A synthesis of the theoretical and simulated maximum directivity obtained for the four antenna arrays is presented in Table I. The theoretical directivity calculated using (11) is equal to 10.4 dBi and 14.3 dBi in the case of the three- and seven-element array, respectively. These results are in good agreement with the maximum directivity calculated from full-wave simulations (10.3 dBi for the three-element array and 15.4 dBi in the case of seven-element array).
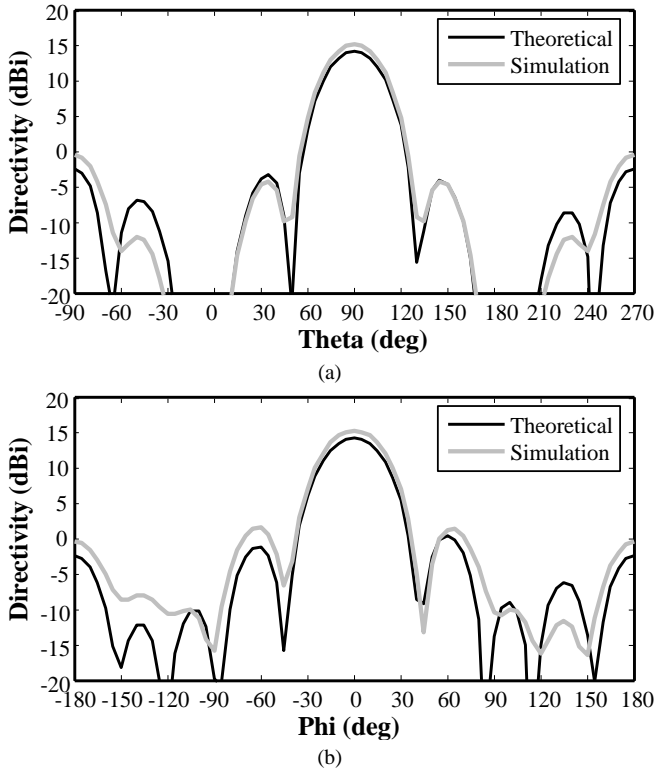

Fig. 3. Theoretical and simulated directivity patterns of the seven-element compact antenna array computed on the (a) E- and (b) H-planes.

In Table I, the theoretical maximum directivity calculated from [13] is also reported. The theoretical and simulated directivity obtained in the case of the three-, four-, and five-

element arrays is very close to this theoretical maximum with an error of about 0.5 dB in the case of the five-element array. The difference obtained in the case of the seven-element array is probably due to the sensitivity of the structure. In fact, due to the reduced inter-element distance ($0.03\lambda_0$) and then to the high mutual coupling between the antenna elements, a small perturbation of the excitation coefficients could produce a relatively significant variation of the array directivity.

The theoretical and simulated directivity patterns obtained for the seven-element array on the E- and H-planes are plotted in Fig. 3. The simulated maximum directivities of the four compact antenna arrays are compared to the theoretical directivity limits in Fig. 4.
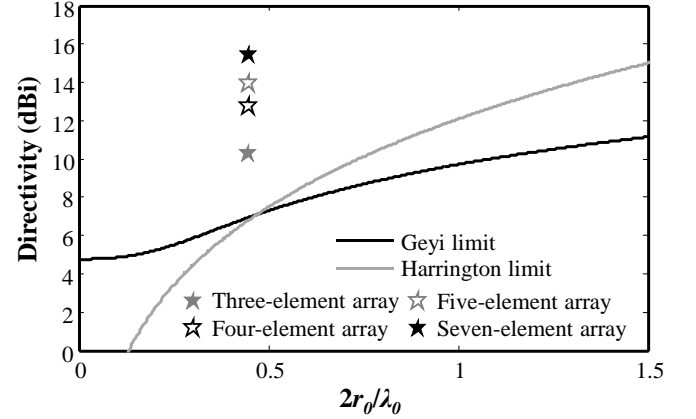

Fig. 4. Maximum simulated directivity of the four compact array antennas compared to the theoretical directivity limits (Harrington [1] and Geyi [2] limits).

In order to study the impact of the super directivity on the antenna efficiency, a four-element array has been optimized as a function of the inter-element distance. The analysis has been computed on the four-element array as in our opinion it constitutes a good trade-off between maximum directivity, sensitivity and fabrication tolerances. The simulated maximum directivity and gain have been plotted in Fig. 5. A gain equal to -8.61 dBi has been achieved when the inter-element distance is equal to $0.07\lambda_0$, while a gain of 11.4 dBi could be obtained with a directivity reduction of 0.5 dB increasing the antenna size (inter-element distance of $0.2\lambda_0$). In conclusion, a compromise between maximum directivity and efficiency must be done [16] depending on the specific application.
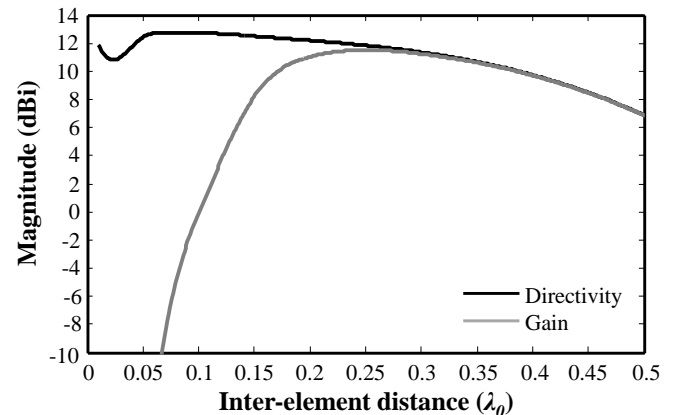

Fig. 5. Theoretical directivity and gain versus the inter-element distance of the four-element super directive array, when the optimal weights are applied.

As our objective is the realization of an efficient spatial filtering function with a compact antenna structure, a four-element array with an inter-element distance of $0.1\lambda_0$ has been demonstrated. Furthermore, it is important to notice that the gain in Fig. 5 has been obtained considering the optimal excitation coefficients calculated using (9). In the practical implementation, additional gain losses are found when the optimal coefficients are implemented using impedance loads.

D. Equivalent impedance load extraction

Using scattering parameters notation, reflection coefficient (Γ) definition and including the excitation vector $\bar{u}$, an equivalent P-port network (see Fig. 2(b) for the two-element case) at a given frequency is described by the equations

$$a_p = \Gamma_p b_p + u_p, \tag{12a}$$

$$b_p = \sum_{j=1}^{P} S_{pj} a_j, \tag{12b}$$

where b_p is the output wave of the $p = 1,..P$ port, S_{pj} are the array S parameters calculated at the STEP 1, Γ_p is the reflection coefficient of the port p and u_p is the excitation term equal to 1 if the feed is located on the port p and equal to 0 in the others cases. It is important to notice that the input wave terms (a_p) in the flow diagram representation (Fig. 2(b)) and in (12a)-(12b) are equal to the excitation coefficients (9) normalized by the coefficient associated to the feed element ($\alpha_p = \alpha_{feed}$). This normalization has been computed in order to have $\Gamma_{feed} = 0$.

Combining (12a)-(12b), the reflection coefficient associated to each array element (port) can be calculated as

$$\Gamma_p = \frac{a_p - u_p}{\sum_{j=1}^{P} S_{pj} a_j}. \tag{13}$$

From (13), the equivalent impedance (Z_p) can be extracted (STEP 4)

$$Z_p = Z_0 \frac{1 + \Gamma_p}{1 - \Gamma_p}. \tag{14}$$

where Z_0 is equal to 50 Ω.

The impedance Z_p can be expressed in terms of discrete loads using the equation

$$Z_p(\omega_{opt}) = R_p + jX_p, \tag{15}$$

where ω_{opt} is calculated at the optimization frequency. R_p and X_p are, respectively, the resistance and the reactance associated to the port p.

IV. APPLICATION TO SUPER DIRECTIVE FOUR-ELEMENT PARASITIC ARRAY DESIGN

In this section, the realized super directive four-element compact array optimization and experimental characterization is presented. The array operates at 868 MHz and consists of four $0.4\lambda_0$ (139.1 mm) electrical dipoles (thickness 2.2 mm) printed on a 124.6 × 156 mm² ($r_0 = 0.28\lambda_0$) Rogers RO4003 substrate (thickness equal to 0.813 mm). The inter-element spacing is $0.1\lambda_0$ (34.6 mm). The schematic view of the

proposed structure is presented in Fig. 6(a). A surface mounted (SMD) balun (Anaren BD0810J50100AHF [28]) has been integrated on a coplanar waveguide and connected to the feed dipole (port 2) in order to obtain a compact balanced excitation. Its characteristics [28] have been taken into account during the array optimization. A photograph of the realized prototype is presented in Fig. 6(b). An impedance matching network has been also integrated on the feed port (Fig. 6(a)). The optimal impedance loads calculated using the proposed optimization procedure has been integrated on each parasitic dipole.
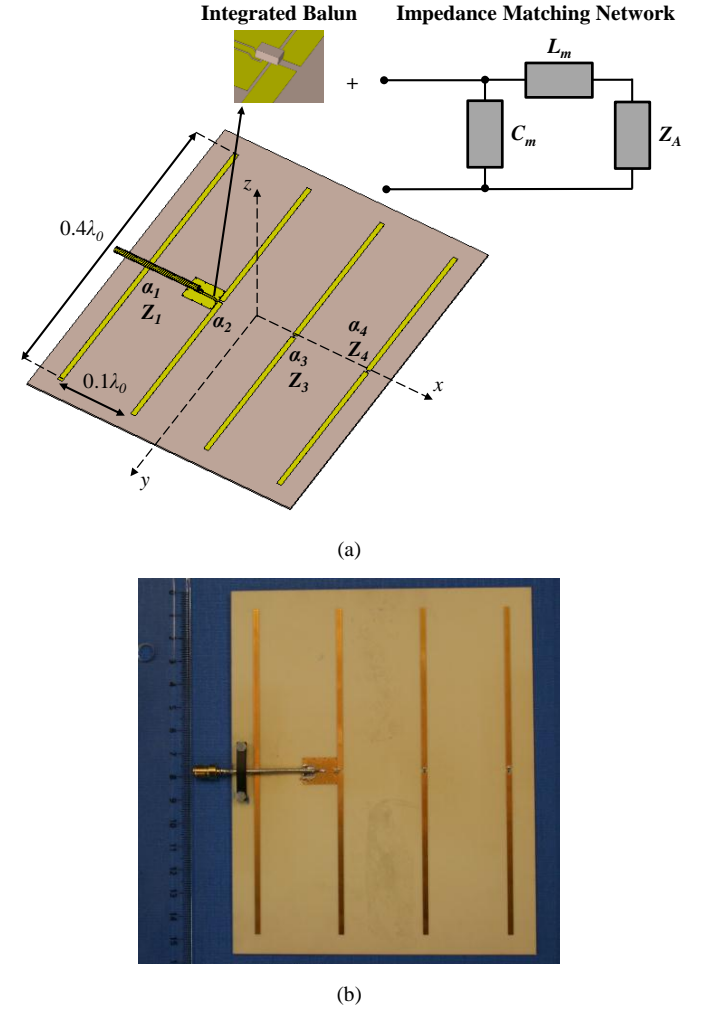

(a)

(b)

Fig. 6. Realized super directive four-element parasitic antenna array. (a) Schematic view of the prototype and of the impedance matching network. (b) Photograph of the antenna.

The optimal excitation coefficients (α_p) (9), equivalent impedances (Z_p) (14), and loads (R_p, L_p) (15) obtained using the proposed synthesis procedure are presented in Table II. A theoretical directivity of 12.6 dBi has been obtained at 868 MHz. The theoretical directivity pattern computed on the E- and H-planes is plotted in Fig. 8. It is important to notice that a negative resistance of -0.16 Ω has been obtained on the port 1 of the array (Table II). Since, the impact of this resistance on the array directivity is negligible (less than 0.2 dB) and the negative resistance implementation discussion is out of the scope of this paper, a resistance R_1 equal to 0 Ω has been used in the practical array implementation.

The compact parasitic antenna array final design has been fully simulated including realistic SMD (standard packaging 0402) component values for the resistances and the inductances. The simulated directivity pattern obtained at 868 MHz is presented in Fig. 8. A maximum directivity of 12.5 dBi has been obtained. The difference between the theoretical and the simulated patterns are probably due to the replacement of the negative resistance and the SMD component realistic values slightly different from the theoretical one.

TABLE II

OPTIMAL WEIGHTS, IMPEDANCES, AND IMPEDANCE LOADS OF THE FOUR-ELEMENT PARASITIC ANTENNA ARRAY COMPUTED WITH THE PROPOSED PROCEDURE AT 868 MHz.

Port	α_p	Z_p	R_p (Ω)	L_p (nH)
1	$0.15e^{-i75.4°}$	-0.16+i25.5	-0.16	4.68
2	$0.36e^{i126.2°}$	50.0	-	-
3	$0.34e^{-i49.4°}$	0.63+i9.51	0.63	1.74
4	$0.14e^{i121.1°}$	1.10+i23.3	1.10	4.27

A. Impedance Matching

Since the input impedance is affected by the interactions between the driven and parasite elements, a matching network has been integrated on the feed port. Due to the definition of the element reflection coefficients (Γ_p) (13), the input impedance can be modified without any effect on the antenna directivity. In our case, we have chosen an L-network in order to realize the matching to 50 Ω. This L-network (Fig. 6(a)) is composed of a series inductance L_m = 1.5 nH and a parallel capacitor C_m = 6.8 pF. The measured reflection coefficient of the realized four-element parasitic antenna array is presented in Fig. 7 and compared to the simulated one. A frequency shift of about 3 MHz has been measured.
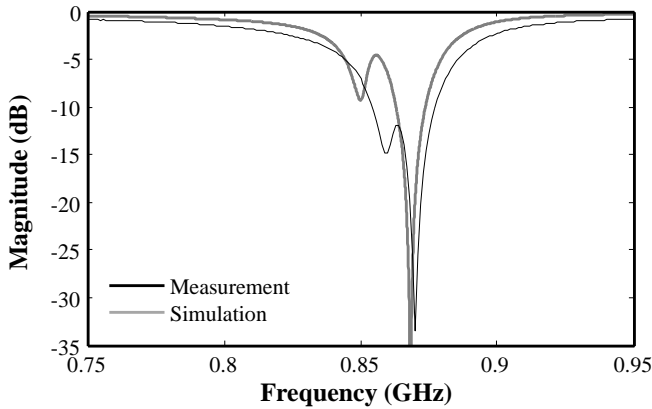

Fig. 7. Measured reflection coefficient of the super directive four-element parasitic antenna array with the impedance matching network.

B. Radiation Pattern Measurements

The radiation properties of the realized four-element compact array have been measured in anechoic chamber. The antenna theoretical (at 868 MHz), simulated (at 868 MHz), and measured (at 871 MHz) directivity patterns computed on two orthogonal planes (E- and H-plane) are plotted in Fig. 8. The corresponding 3-dB beamwidths are presented in Table III. A maximum directivity of 11.7 dBi has been measured in satisfactory agreement with theory (12.6 dBi) and full-wave

simulation (12.5 dBi). The simulated and measured maximum directivity and realized gain as a function of the frequency are also presented in Fig. 9. A 1-dB directivity bandwidth of 5.5 MHz around 871 MHz has been measured. A satisfactory agreement between simulation and measurement has been obtained with a slight frequency shift of about 3 MHz. The discrepancy between the simulated and the measured results can be principally attributed to the tolerances of the discrete loads used to implement the impedance matching network and the excitation coefficients (±5% for the resistances and ±0.2 nH for the inductances).
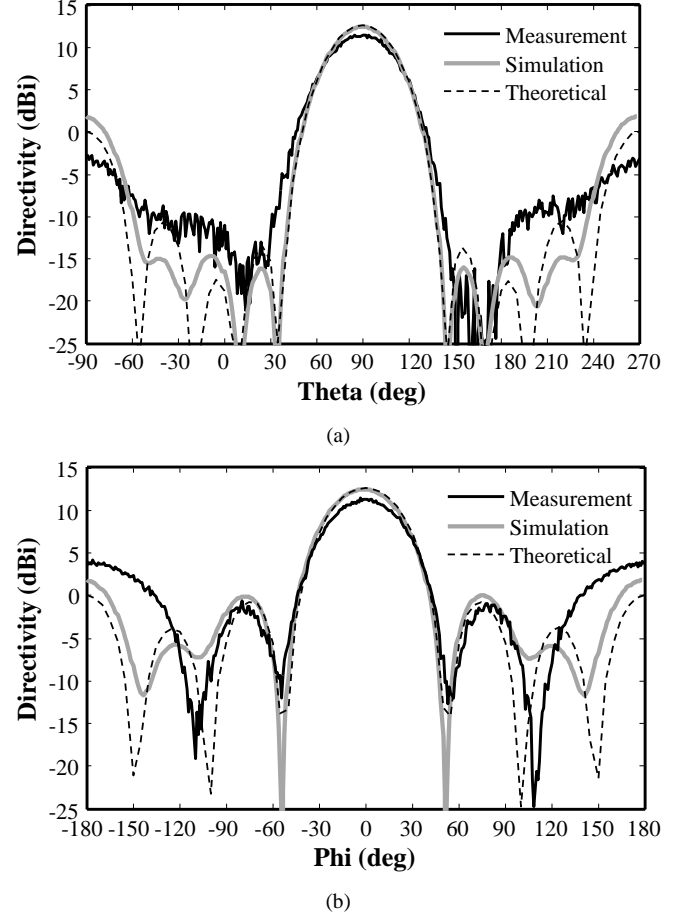

(a)

(b)

Fig. 8. Theoretical (868 MHz), simulated (868 MHz), and measured (871 MHz) directivity pattern of the realized super directive four-element parasitic antenna array. (a) E- and (b) H-plane.

The measured (871 MHz) and simulated (868 MHz) gain is equal to -12.0 dBi and -15.3 dBi, respectively. These values must be compared with the theoretical gain (-0.15 dBi) presented in Fig. 5. The losses have been analyzed by full-wave simulation. They are principally due to the resistive loads used to implement the optimal excitation coefficients (around -4 dB) and the intrinsic resistance of the balun integrated on the feed port (around -8.5 dB considering a 3 Ω resistance). Avoiding resistive loads and considering pure reactive ones (Table II) a directivity of 11.1 dBi (12.5 dBi with resistances) has been obtained with a gain of -18.0 dBi.

V. CONCLUSION

In this paper, a new procedure to design and optimize super directive parasitic antenna arrays has been presented. The

procedure is based on spherical wave expansion and can be used to optimize the antenna directivity independently from the beam direction, antenna geometry, and chosen polarization. The theoretical analysis shows that a maximum end-fire super directivity of 10.4, 12.5, 13.8, and 14.3 dBi can be obtained using three, four, five, and seven half-wavelength dipole arrays ($r_0 = 0.22\lambda_0$) in excellent agreement with Uzkov's theory [12],[13].
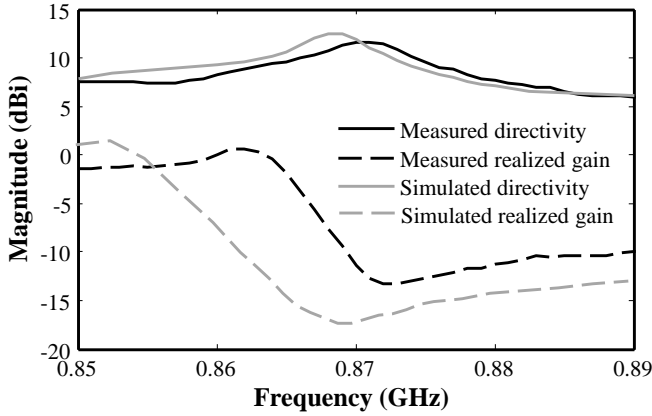

Fig. 9. Simulated and measured directivity and realized gain of the four-element parasitic antenna array as function of the frequency.

TABLE III

THEORETICAL (868 MHz), SIMULATED (868 MHz), AND MEASURED (871 MHz) PERFORMANCES OF THE PROPOSED SUPER DIRECTIVE FOUR-ELEMENT COMPACT ARRAY.

	Directivity (dBi)	3-dB beamwidth (°, H-plane)	3-dB beamwidth (°, E-plane)
Theoretical	12.6	41.0	46.4
Simulation	12.5	41.2	46.7
Measurement	11.7	45.0	47.0

In order to validate the design procedure and the theoretical results, a super directive four-element compact parasitic antenna array ($r_0 = 0.28\lambda_0 = \lambda_0/3.6$) has been designed, optimized, manufactured, and experimentally characterized. A maximum end-fire super directivity of 11.7 dBi has been measured in satisfactory agreement with the theory and full-wave simulation. In our best knowledge, this is the first practical demonstration of a super directive four-element compact array in the open literature. Future studies will investigate the possibility to ameliorate the antenna efficiency.

REFERENCES

[1] R. F. Harrington, "On the gain and beamwidth of directional antennas," *IEEE Trans. Antennas Propag.*, vol. 6, no.3, pp. 219-225, Jul. 1958.

[2] W. Geyi, "Physical limitations of antenna," *IEEE Trans. Antennas Propag.*, vol. 51, no. 8, pp. 2116-2123, Aug. 2003.

[3] L. J. Chu, "Physical limitations on omni-directional antennas," *J. Appl. Phys.*, vol. 19, pp. 1163-1175, Dec. 1948.

[4] R. Collin, and S. Rothschild, "Evaluation of antenna Q," *IEEE Trans. Antennas Propag.*, vol. 12, no. 1, pp. 23-27, Jan. 1964.

[5] J. S. McLean, "A re-examination of the fundamental limits on the radiation Q of electrically small antenna," *IEEE Trans. Antennas Propag.*, vol. 44, no. 5, pp. 672-676, May 1996.

[6] D. Pozar, "New results for minimum Q, maximum gain, and polarization proprerties of electrically small antennas," *3rd European Conf. Antennas Propag. (EuCAP 2009)*, Mar. 2009.

[7] A. D. Yaghjian, and S. R. Best, "Impedance, bandwidth, and Q of antennas" *IEEE Trans. Antennas Propag.*, vol. 53, no. 4, pp. 1298-1324, Apr. 2005.

[8] S. R. Best "The radiation properties of electrically small folded spherical helix antennas," *IEEE Trans. Antennas Propag.*, vol. 52, no. 4, pp. 953-960, Apr. 2004.

[9] A. Erentok, and R. W. Ziolkowski, "Metamaterial – inspired efficient electrically small antennas," *IEEE Trans. Antennas Propag.*, vol. 56, no. 3, pp. 691-707, Mar. 2008.

[10] O. S. Kim, O. Breinbjerg, and A. D. Yaghjian, "Electrically small magnetic dipole antennas with quality factors approaching the Chu lower bound," *IEEE Trans. Antennas Propag.*, vol. 58, no. 6, pp. 1898-1906, Jun. 2010.

[11] A. D. Yaghjian, "Lower bounds on the Q of electrically small dipole antennas," *IEEE Trans. Antenna Propag.*, vol. 58, no. 10, Oct. 2010.

[12] A. I. Uzkov, "An approach to the problem of optimum directive antennae design," *Comptes Rendus de l'Académie de Sciences de l'URSS*, vol. 53, no. 1, pp. 35-38, 1946.

[13] E. E. Altshuler, T. H. O'Donnell, A. D. Yaghjian, and S. R. Best, "A monopole superdirective array," *IEEE Trans. Antennas Propag.*, vol. 53, no. 8, pp. 2653–2661, Aug. 2005.

[14] S. R. Best, E. E. Altshuler, A. D. Yaghjian, J. M. McGinthy, and T. O'Donnell "An impedance-matched 2-element superdirective array," *IEEE Antennas and Wireless Propag. Lett.*, vol. 7, pp. 302-305, 2008.

[15] M. Lancaster, Z. Wu, Y. Huang, T. S. M. McClean, X. Zhou, G. Gough, and N. McN Alford, "Superconducting antennas," *Supercond. Sci. Technol.* Vol. 5, pp. 227-279, 1992.

[16] O. S. Kim, S. Pivnenko, and O. Breinbjerg, "Superdirective magnetic dipole array as first-order probe for spherical near field antenna measurements," *IEEE Trans. Antennas Propag.*, vol. 60, no. 10, pp. 4670-4676, Oct. 2012.

[17] D. R. Bowling, D. J. Banks, D. M. Kinman, and A. M. Martin, "A three-element, superdirective array of electrically small, high-temperature superconducting halh-loops at 500-MHz," in *Proc. Int'l Symp. Antennas Propagat.,* Ann Arbor, MI, USA, Jun. 28-Jul. 2, 1993, vol. 3, pp. 1846-1849.

[18] Z. Bayraktar, P.L. Werner, and D.H. Werner, "The design of miniature three-element, stochastic Yagi-Uda arrays using particle swarm optimization," *IEEE Antennas Wireless Propagat. Letts.*, vol. 5, pp. 22–26, Dec. 2006.

[19] S. Lim and H. Ling, "Design of a closely spaced, folded Yagi antenna," *IEEE Antennas Wireless Propagat. Letts.*, vol. 5, pp. 302–305, Dec. 2006.

[20] M. Pigeon, C. Delaveaud, L. Rudant, and K. Belmkaddem, "Miniature directive antennas," *Intern. J. Microwave Wireless Techn.*, vol. 6, special issue 1, pp. 45-50, Feb. 2014.

[21] A. Clemente, M. Pigeon, L. Rudant, and C. Delaveaud, "Super directive compact antenna design using spherical wave expansion," in *Proc. IEEE Antennas Propag. Soc. Int. Symp.*, Memphis, TN, Jul. 6-11, 2014.

[22] J. E. Hansen, "Spherical near-field antenna measurements," *IET Electromag. Waves Series*, 1988.

[23] F. Jensen, "Electromagnetic near-field far-field correlations," *PhD thesis at Laboratory Electromagnetic Theory*, *Technical University of Denmark*, Jul. 1970.

[24] H. L. Thal Jr., and J. B. Manges, "Theory and practice for a spherical-scan near-field antenna range," *IEEE Trans. Antennas and Propag.*, vol. 36, no. 6, pp. 815-821, Jun. 1988.

[25] I. J. Gupta, and A. A. Ksienski, "Effect of mutual coupling on the performance of adaptive arrays," *IEEE Trans. Antennas Propag.*, vol. 31, no. 5, pp. 785–791, May 1983.

[26] M. Thevenot, C. Menudier, A. El Sayed Ahmad, G. Zakka El Nashef, F. Fezai, Y. Abdallah, E. Arnaud, F. Torres, and T. Monediere, "Synthesis of antennas arrays and parasitic antenna arrays with mutual coupling," *Intern. J. Antennas Propag.*, 2012.

[27] F. Fezai, C. Menudier, M. Thevenot, and T. Monediere, "Systematic design of parasitic element antennas – Application to a WLAN Yagi Design," *IEEE Antennas and Wireless Propag. Lett.*, vol. 12, pp. 413-416, 2013.

[28] Anaren "B0310J50100AHF xinger balun," 2014 [On-line] Available http://www.anaren.com/sites/default/files/B0310J50100AHF_DataSheet_RevA.pdf.

Antonio Clemente received the B.S. and M.S. degree in telecommunication engineering and remote sensing systems from the University of Siena, Italy, in 2006 and 2009, and the Ph.D. degree in signal processing and telecommunications from the University of Rennes 1, France, in 2012. From October 2008 to May 2009 he realized his master thesis project at Technical University of Denmark (DTU), Lyngby, Denmark, where he worked on spherical near-field antenna measurements. His Ph.D. has been realized at CEA-LETI, Grenoble, France. In 2012, he joined the R&D laboratory of Satimo Industries, Villebon-sur-Yvette, France. Since 2013, he is a Research Engineer at CEA-LETI, Grenoble, France. His current research interests include quasi-optic reconfigurable antennas at microwave and millimeter-wave frequencies, miniature integrated antennas, near-field and far-field antenna measurements.
Dr. Clemente received the Young Scientist Awards (First Prize) during the 15th International Symposium of Antenna Technology and Applied Electromagnetics 2012 (ANTEM 2012) in Toulouse, France.

Melusine Pigeon received a degree in engineering from the National School of Civil Aviation (ENAC), Toulouse, France, in 2007 and her Ph.D. degree in Microwave, Electromagnetism and Optoelectronics in 2011. After holding different post-doctoral position at the CEA-Leti, Grenoble, France, and at the IETR (Institut d'électronique et de télécommunications de Rennes), Rennes, France, she now holds a post-doctoral fellowship at the Queen Mary University of London, UK. Her main research interests include antennas at Terahertz frequencies, compact antennas, metamaterials, and antenna fundamental limitations.

Lionel Rudant prepared national selective exams in Saint-Denis, Reunion Island, France. He received the Electronic and Digital Technologies Engineering degree from Polytech'Nantes, the Graduate School of the University of Nantes, France, in 2003. In 2004, he received the Technology Research Engineering degree from Grenoble Institute of Technology, Grenoble, France.In 2004 and 2005; he was in charge of antenna projects for automotive in European research center of Radiall-Larsen Antenna Technology in Voiron, France. In 2006, he joined the Laboratory of Electronics and Information Technology (Leti), Grenoble, France. His main interests include small antenna design, MIMO antennas for terminals, Over-The-Air tests, reconfigurable antennas, superdirectivity. Since 2012, he is in charge with strategic programs and industrial partnerships for Leti activities in the field of wireless systems.

Christophe Delaveaud completed a university curriculum resulting in a PhD in Optical Communication and Microwave Techniques obtained in 1996 at the University of Limoges. After industrial experience in company Radiall (Voreppe, France), he joined in 2002 the Electronic and Information Technology Laboratory of the French Atomic Energy and Alternatives Energy Commission (CEA-Leti) based in Grenoble (France). After his appointment as senior expert in 2003, he obtained his Accreditation to Direct Physics Research at the University Joseph Fourrier, Grenoble (2010). His research areas range from electromagnetism applied to antennas (miniature antennas, multi-antenna systems, reconfigurable antennas), to propagation and microwave circuits for radio frequency transmitters. Since 2012, he heads the Antennas and Propagation Laboratory of CEA-LETI. To date, C. Delaveaud has contributed to more than 170 papers and communications in major revues and conferences in the field of antennas and radio frequency circuits, and is the author or co-author of 15 patents of invention.